Application of Potent Potential Functions in Eye/Head Movement Control

Bijoy K. Ghosh and Indika Wijayasinghe

Abstract— **In this paper we study the human eye movement and the head movement system as a simple mechanical control system. Most of the time, eye movements obey Listing's constraint, which states that the allowed orientations of the eye are obtained by rotating a fixed 'primary gaze direction' by a subclass of rotation matrices. These rotation matrices have their axes of rotation restricted to a fixed plane perpendicular to the primary gaze direction. Likewise, a spontaneous head movement satisfy Donder's constraint which is similar to the Listing's constraint except that the axes of rotation of the head away from a primary head position is restricted to a fixed surface, which is not necessarily a plane. When head is restrained to remain fixed, eye movement satisfies the Listing's constraint throughout its entire trajectory. On the other hand, when the head is allowed to move (satisfying the Donder's constraint), the eye satisfies the Listing's constraint only at the beginning and at the end of a trajectory. Intermediate points of the trajectory, partially guided by the vestibulo-ocular reflex, do not apparently satisfy the Listing's constraint. In this paper we introduce control strategy that would regulate the eye from an initial to a final gaze position with or without satisfaction of the Listing's constraint during all the intermediate points of the eye movement trajectory. We study the head movement problem under the assumption that the head always satisfies the Donder's constraint. The control signals are generated by choosing a suitable potential function and adding to it a suitable damping term. The overall dynamical system is constructed using the well known Euler Lagrange's equation. The main result of this paper is to compare, using simulations, the total distance and the total time it takes to regulate the eye and the head between two orientations.**

I. Introduction

Modeling the eye in order to generate various eye movements has been one of the important goals among neurologists, physiologists and engineers since 1845 (see the work of Listing, Donders and Helmoltz etc in [12]). Previous studies which used modeling as a means of understanding the control of the eye movements have adopted two main approaches. (see [6] and [11]. In spite of several notable studies of three dimensional eye movements [1], [5], with the exception of some recent papers in the subject [9], [15], there has not been a rigorous treatment of the topic in the framework of modern control theory and geometric mechanics. Assuming the eye to be a rigid sphere, the problem of eye movement can be treated as a mechanical control system [3], [8] and the results of classical mechanics can be promptly applied.

Most of the earlier studies in eye movement assumed that the head remained fixed and the eye is allowed to move freely. It was observed by Listing (see [13]), that in this situation the orientation of the eye was completely determined by its gaze direction. Subsequently it was shown that starting from a frontal gaze, any other gaze direction is obtained by a rotation matrix whose axis of rotation is constrained to lie on a plane, called the Listing's Plane. Consequently, the set of all orientations the eye can assume is a submanifold of $\mathbf{SO}(3)$ (see Boothby [2] for a definition) called **LIST**. Listing showed that in a head fixed environment, eye orientations are restricted to this specific submanifold **LIST**.

In this paper, we are interested in the study of eye movement when head is allowed to move as well. To fix our ideas, assume that the head can move spontaneously on the torso and the eye moves with respect to the head coordinate. Assume that our goal is to fixate on a stationary target on the visual space observed at a certain angle from the initial gaze direction. In this situation, as was described by Tweed [14], the eye moves rapidly towards the target, violating the Listing's constraint. However, even under this motion, the initial and the final orientation of the eye is on the submanifold **LIST**. The head, in the mean time, moves spontaneously towards the object as well, following a Listing like constraint that goes by the name Donder's constraint [7], [10].

Donder's law states that starting from a frontal head position, any other head orientation is obtained by a rotation matrix whose axis of rotation is constrained to lie on a two dimensional surface, called the Donder's Surface [14]. Consequently, the set of all orientations the head can assume spontaneously is a submanifold of $\mathbf{SO}(3)$ called **DOND**. We would like to remark that unlike the eye, head can be oriented voluntarily outside the submanifold **DOND**. For simplicity, we shall not detail this voluntary action in this paper.

Simultaneous movement of the eye and the head to fixate on a target, either stationary or moving, is a subject of intense research (see [4]). The basic approach of this paper is an extension of our earlier paper [9].

Bijoy K. Ghosh is the Director of Laboratory for BioCybernetics and Intelligent Systems, Texas Tech University, Lubbock, Texas 79409, USA. bijoy.ghosh@ttu.edu Indika Wijayasinghe is with the Department of Mathematics and Statistics Texas Tech University, Lubbock, Texas 79409, USA indika.wijayasinghe@ttu.edu

II. Riemannian Metric on SO(3), LIST and DOND

It has been described in [9] that eye rotations are typically confined to a sub manifold **LIST** of **SO**(3) especially when the head is restrained to be fixed. In order to write down the equations of motion, one needs to know the kinetic and the potential energies of the eye in motion. The kinetic energy is given by the induced Riemannian metric on **LIST**, induced from the Riemannian metric on **SO**(3). The Riemannian metric is derived from the moment of inertia of the eye ball. We assume that the eye is a perfect sphere and its inertia tensor is equal to $I_{3\times 3}$. This is associated with a left invariant Riemannian metric on **SO**(3) given by

$$< \Omega(e_i), \Omega(e_j) >_I = \delta_{i,j}, \tag{1}$$

where

$$\Omega(e_k) = \begin{pmatrix} 0 & \delta_{3,k} & -\delta_{2,k} \\ -\delta_{3,k} & 0 & \delta_{1,k} \\ \delta_{2,k} & -\delta_{1,k} & 0 \end{pmatrix} \tag{2}$$

and $\delta_{l,m}$ denotes the Kronecker delta function. An easy way to carry out computation using this Riemannian metric is provided by an isometric submersion **rot** between $\mathbf{S}^3$ and **SO**(3)

$$\mathbf{S}^3 \stackrel{\mathbf{rot}}{\rightarrow} \mathbf{SO}(3) \tag{3}$$

The map **rot** has already been described in [9]. Let us now define a coordinate map on $\mathbf{S}^3$ as follows:

$$\rho : [0,\pi] \times [0,2\pi] \times \left[-\frac{\pi}{2}, \frac{\pi}{2}\right] \rightarrow S^3 \tag{4}$$

where

$$\rho(\theta,\phi,\alpha) = \begin{pmatrix} \cos(\phi/2) \\ \sin(\phi/2)\ \cos(\theta)\ \cos(\alpha) \\ \sin(\phi/2)\ \sin(\theta)\ \cos(\alpha) \\ \sin(\phi/2)\ \sin(\alpha) \end{pmatrix} \tag{5}$$

The composition mapping $\mathbf{rot} \circ \rho(\theta,\alpha,\phi)$ is a rotation around the axis

$$\begin{pmatrix} \cos\theta\ \cos\alpha \\ \sin\theta\ \cos\alpha \\ \sin\alpha \end{pmatrix} \tag{6}$$

by a counterclockwise angle ϕ. Note in particular that when $\alpha = 0$, the axis of rotation is restricted to a plane, known as the Listing's plane. The angle θ measures the angle of the axis on the Listing's plane and the angle α measures deviation of the axis from the Listing's Plane. The Riemannian metric on **SO**(3) is given by:

$$g = \sin^2(\phi/2)\cos^2(\alpha)\,d\theta^2 + \sin^2(\phi/2)\,d\alpha^2 + \frac{1}{4}d\phi^2. \tag{7}$$

Restricted to the Listing's plane, i.e. when $\alpha = 0$, the Riemannian metric on **LIST** is given by

$$g = \sin^2(\phi/2)\,d\theta^2 + \frac{1}{4}d\phi^2 \tag{8}$$

as has been already described in [9]. The submanifold **DOND** is described by restricting

$$\alpha = \varepsilon \sin(2\theta), \tag{9}$$

where ε is a small parameter. The Riemannian metric on **DOND** is computed to be

$$g = \sin^2\frac{\phi}{2}\left[\cos^2\alpha + \left(\frac{\partial\alpha}{\partial\theta}\right)^2\right] d\theta^2 + \frac{1}{4}\,d\phi^2. \tag{10}$$

Using the Riemannian metric (7) for **SO**(3), it is a straightforward but tedious computation to show that the associated geodesic equation is given by

$$\begin{aligned} \ddot{\theta} + \dot{\theta}\dot{\phi}\cot(\phi/2) + \dot{\theta}\dot{\alpha}\tan(\alpha) &= 0 \\ \ddot{\phi} - \left(\dot{\theta}\right)^2\sin(\phi)\cos^2(\alpha) - (\dot{\alpha})^2\sin(\phi) &= 0 \\ \ddot{\alpha} + \frac{1}{2}\left(\dot{\theta}\right)^2\sin(2\alpha) + \dot{\phi}\dot{\alpha}\cot(\phi/2) &= 0. \end{aligned} \tag{11}$$

When $\alpha = 0$, the above geodesic equation (11) reduces to the following pair of equations already described in [9] given by

$$\begin{aligned} \ddot{\theta} + \dot{\theta}\dot{\phi}\cot(\phi/2) &= 0 \\ \ddot{\phi} - \left(\dot{\theta}\right)^2\sin(\phi) &= 0. \end{aligned} \tag{12}$$

The geodesic equation (12) can also be directly computed from the Riemannian metric (8) on the submanifold **LIST** of **SO**(3).

Finally, the geodesic equation on **DOND** can be computed as follows.

$$\begin{aligned} \left[\cos^2\alpha + \left(\frac{\partial\alpha}{\partial\theta}\right)^2\right]\ddot{\theta} - \frac{\partial\alpha}{\partial\theta}\left[\left(\frac{\partial^2\alpha}{\partial\theta^2} - \frac{1}{2}\sin(2\alpha)\right)\dot{\theta}^2\right] &= 0 \\ \ddot{\phi} - \left(\dot{\theta}\right)^2\sin(\phi) &= 0. \end{aligned} \tag{13}$$

where α is defined as in (9).

III. General Equation of Motion

The Riemannian Metrics that we had obtained so far in (7), (8) and (10) enables us to write down an expression for the kinetic energy KE. In general, the dynamics is affected by an additional potential energy and an external input torque. Let us consider a general form of the potential function given by

$$V(\theta,\phi,\alpha) = A\,\sin^2\frac{\phi}{2} + B\,\cos^2\frac{\phi}{2}\,\sin^2\alpha. \tag{14}$$

The expression for the Lagrangian is given by

$$L = KE - V, \tag{15}$$

and the equation of motion is described by

$$\frac{d}{dt}\left(\frac{\partial L}{\partial\dot{\beta}}\right) - \left(\frac{\partial L}{\partial\beta}\right) = \tau_\beta \tag{16}$$

where β is the angle variable.

A. Motion satisfying the Listing's Constraint

The Listing's constraint is satisfied when $\alpha = 0$ and the kinetic energy is given by

$$KE \;=\; \frac{1}{2}\left[\sin^2\frac{\phi}{2}\,\dot{\theta}^2 \;+\; \frac{1}{4}\dot{\phi}^2\right].$$

The following motion equation follows easily from the Euler-Lagrange equation given by

$$\begin{aligned} \ddot{\theta} + \dot{\theta}\dot{\phi}\cot(\phi/2) &= \csc^2(\phi/2)\,\tau_\theta \quad (17)\\ \ddot{\phi} - \left(\dot{\theta}\right)^2\sin(\phi) + 2\mathrm{A}\sin(\phi) &= 4\tau_\phi. \end{aligned}$$

B. Motion that does not satisfy the Listing's Constraint

When α is unrestricted, Listing constraint is not satisfied and the rotation matrix remains unrestricted in $\mathbf{SO}(3)$. In this case, the kinetic energy is given by

$$KE \;=\; \frac{1}{2}\left[\sin^2\frac{\phi}{2}\cos^2\alpha\dot{\theta}^2 \;+\sin^2\frac{\phi}{2}\dot{\alpha}^2 + \frac{1}{4}\dot{\phi}^2\right]. \qquad (18)$$

One can now obtain the following equation from the Euler Lagrange's equation.

$$\begin{aligned} \ddot{\theta} &= 2\tan\alpha\,\dot{\alpha}\,\dot{\theta} \;-\; \dot{\theta}\,\dot{\phi}\,\cot\frac{\phi}{2} \;+\csc^2\frac{\phi}{2}\,\sec^2\alpha\,\tau_\theta\\ \ddot{\phi} &= \sin\phi\left[\cos^2\alpha\,\dot{\theta}^2 \;+\; \dot{\alpha}^2 \;-\; 2A\right] \;+\; 4B\,\sin\phi\,\sin^2\alpha \;+4\,\tau_\phi\\ \ddot{\alpha} &= -\cot\frac{\phi}{2}\,\dot{\alpha}\,\dot{\phi} \;-\; \frac{1}{2}\,\sin(2\alpha)\,\dot{\theta}^2 \;+\; \left[\tau_\alpha \;-\; B\,\cos^2\frac{\phi}{2}\,\sin(2\alpha)\right]\csc^2\frac{\phi}{2}. \end{aligned}$$

C. Motion satisfying the Donder's Constraint

We have already noted that the Donder's constraint is obtained by setting the angle α as in (9). This way, although the torsional component of the rotation is slightly nonzero, it is completely specified by the angle θ. We choose the kinetic and the potential energy as (18) and (14) respectively. We now obtain the following equation from Euler Lagrange's equation.

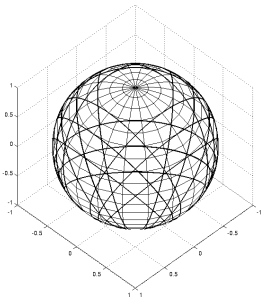

(a) North Pole is the frontal gaze direction

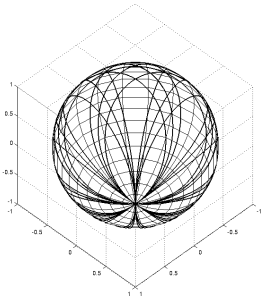

(b) South Pole is the backward gaze direction

Fig. 1: Geodesics for equation (12) for eye movement that satisfies Listing's Law.

In plotting the figure, we have chosen the convention that the identity rotation matrix corresponds to the frontal gaze. Our simulations show that all geodesics are circles that pass through the backward gaze which is physically unattainable.

$$\begin{aligned} \frac{d}{dt}\left[\sin^2\frac{\phi}{2}\left(\cos^2\alpha + \left(\frac{\partial\alpha}{\partial\theta}\right)^2\right)\dot{\theta}\right] \;-\; \sin^2\frac{\phi}{2}\,\dot{\theta}^2\,\frac{\partial\alpha}{\partial\theta}\left[\frac{\partial^2\alpha}{\partial\theta^2} \;-\; \frac{1}{2}\,\sin(2\alpha)\right] &= -B\,\cos^2\frac{\phi}{2}\,\sin(2\alpha)\,\frac{\partial\alpha}{\partial\theta} \;+\; \tau_\theta\\ \ddot{\phi} \;-\; \left[\cos^2\alpha \;+\; \left(\frac{\partial\alpha}{\partial\theta}\right)^2\right]\dot{\theta}^2\,\sin\phi = -2A\sin\phi \quad + \quad 2B\sin^2\alpha\,\sin\phi \;+\; 4\tau_\phi, \qquad (19) \end{aligned}$$

where we continue to assume that α satisfies the Donder's constraint (9).

IV. Examples

In all, six examples are considered that relate to the eye and the head movement problems.

Example 1 (Eye Movement Geodesic): In this example we solve the geodesic equation (12) (corresponds to eye rotation that satisfy the Listing's constraint) and show in Fig. 1 that the geodesic curves are circles passing through a fixed point. In Fig. 1 we have plotted the gaze directions as a function of time starting from different initial conditions.

Example 2 (Restricted Eye Movement with a potential function): In this example we solve the motion equation (17) (corresponds to eye rotation that satisfy the Listing's constraint) and show the gaze trajectories in Fig. 2. We have assumed $\tau_\theta = \tau_\phi = 0$, and increasing magnitudes A of the potential function has been chosen. Our simulations show that with increasing magnitude of the potential function, the gaze trajectories are restricted to a smaller neighborhood of $\phi = 0$, the frontal gaze. The main message of this example is that the region of the eye movement trajectories can be restricted by a suitable choice of the potential function.

In the next example we show that by adding a friction

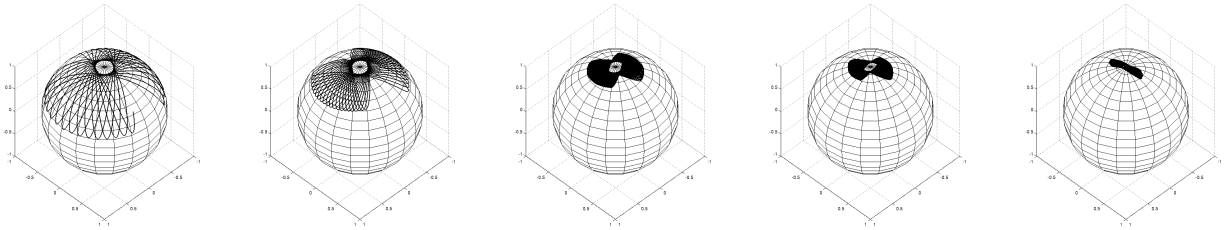

(a) A = 0.5 (b) A = 1 (c) A = 5 (d) A = 10 (e) A = 50

Fig. 2: Eye movement under the influence of a potential function, using equation (17) with $\tau_\theta = \tau_\phi = 0$. The parameter A is the amplitude of the potential function.

term, the gaze trajectories can be made to converge to the point of minimum potential energy. This strategy will subsequently be used to direct the final position of the gaze.

Example 3 (Damped eye movement trajectories minimizing a potential function): We remark that in example 2, one of the properties of the eye movement trajectory is that with increasing amplitude A of the potential function the gaze trajectories are restricted to the frontal part of the visual field, a desirable feature. Unfortunately, we observe that the trajectories themselves are increasingly jittery. In this example we repeat example 2 but choose $\tau_\theta = -k\,\dot{\theta}$ and $\tau_\phi = -k\,\dot{\phi}$ in order to dampen the trajectories. The results are plotted in Fig. 3.

Example 4 (Head Free Eye Movement when Listing's constraint is not satisfied): We modify the potential function (14) and choose

$$V(\theta,\phi,\alpha) = A\,\sin^2\left[\frac{\theta(t)-\theta_f}{2}\right] + B\,\sin^2\left[\frac{\phi(t)-\phi_f}{2}\right] + C\,\cos^2\left[\frac{\theta(t)-\theta_f}{2}\right]\cos^2\left[\frac{\phi(t)-\phi_f}{2}\right]\,\sin^2\left[\alpha(t)-\alpha_f\right]. \quad (20)$$

The angles θ_f, ϕ_f and α_f are constants indicating the desired final values of the angles θ, ϕ and α. The potential function is minimized at $\theta = \theta_f$, $\phi = \phi_f$, $\alpha = \alpha_f$, indicating that when $\alpha_f = 0$ the potential is minimized when the Listing's constraint is satisfied. The special form of the potential function (20) ensures that $\alpha(t)$ is close to α_f near the end of the trajectory.

We vary α_f both in the positive and negative directions away from 0. For every choice of α_f, we alter both θ_f and ϕ_f in such a way that the final gaze direction of the eye remains unaltered, although the final orientations are not the same. By deviating away from the Listing's constraint, we show in this example that there is an optimum choice of α_f (about 0.5), for which the total trajectory distance is minimized. Likewise there is another optimum choice of α_f (about 1.0,) for which the elapsed time for the gaze transfer is minimum.

This example illustrates the point that when eye has to move rapidly to capture a target, **it pays to deviate from the Listing's constraint.** Once the target is captured, α_f is reset to 0 rapidly by the vestibuloocular reflex.

Example 5 (Head movement Geodesic): In this example we solve the geodesic equation (13) (corresponds to head rotation that satisfy the Donder's constraint) and show in Fig. 5 that the geodesic curves are close to a circle for small values of the perturbation parameter ε. In Fig. 5 we have plotted the gaze directions as a function of time for a fixed initial condition and for three different values of ε. In plotting the figure, we have chosen the convention that the identity rotation matrix corresponds to the frontal head position.

Example 6 (Head movement connecting an initial and final head direction): In this final example, we display head movement satisfying Donder's constraint and consider a modified form of the potential function described as

$$V(\theta,\phi) = A\,\sin^2\left[\frac{\theta(t)-\theta_f}{2}\right] + B\,\sin^2\left[\frac{\phi(t)-\phi_f}{2}\right]. \quad (21)$$

The angle $\alpha(t)$ is constrained to satisfy $\alpha(t) = \varepsilon\,\sin(2\theta(t))$ at all times. We also add a frictional term proportional to the negative derivatives of θ and ϕ. In this example, the initial and the final values of θ and ϕ are chosen in such a way that for every trajectory, the head moves from one fixed head direction to another fixed head direction. The results are displayed in Fig. 6 for three different choices of ε.

We note from Fig. 7 that for a larger value of ε, i.e. when a larger torsion is allowed during head movement, the total distance the head has to move is rising. This is understandable since there is an extra head rotation for the same head direction. Surprisingly, the time to complete the trajectory seems to fall as a function of ε indicating that perhaps – **it pays to slightly rotate your head.**

V. Conclusion

In general, it is important to be able to move between two gaze positions using a trajectory that is restricted to within a

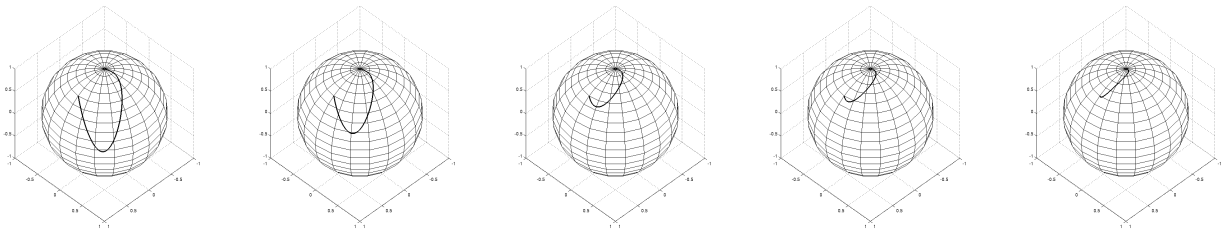

(a) A = 0.5 (b) A = 1 (c) A = 5 (d) A = 10 (e) A = 50

Fig. 3: Eye movement under the influence of a potential function and a constant friction term using equation (17) with $\tau_\theta = -k\,\dot{\theta}$ and $\tau_\phi = -k\,\dot{\phi}$. The value of k is chosen to be 0.1.

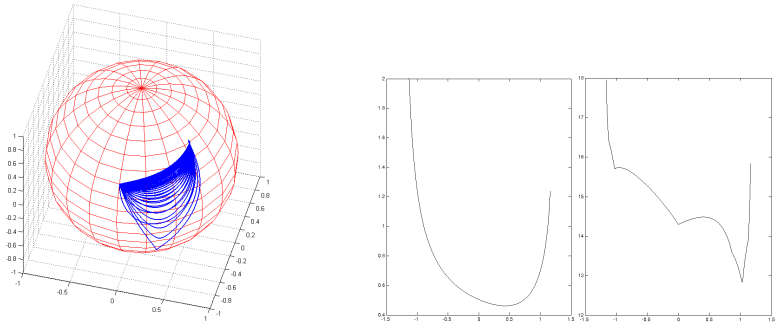

(a) Gaze Space Trajectory (b) Trajectory Distance vs. α_f (c) Elapsed Time vs. α_f

Fig. 4: Eye Movement under different choices of α_f

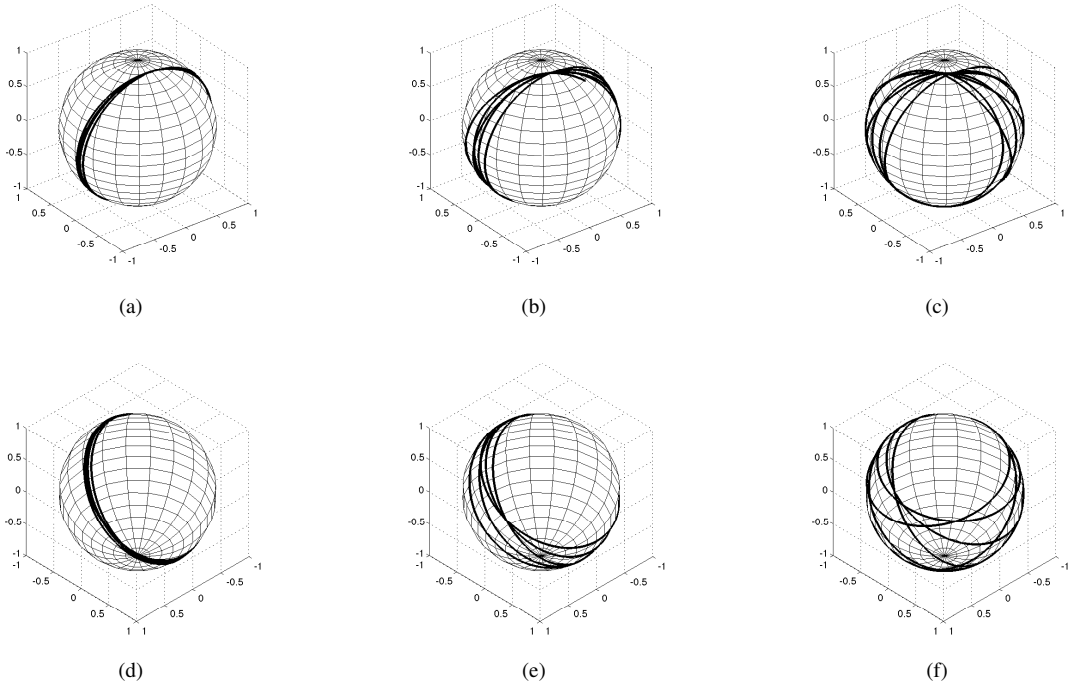

(a) (b) (c) (d) (e) (f)

Fig. 5: Geodesics for equation (13) for head movement that satisfies Donder's Law. In each of the figures the north pole is the frontal position of the head (top three figures), and the south pole is the backward head position (bottom three figures). The values of ε are given by 0.1, 0.2 and 0.3 from left to right.

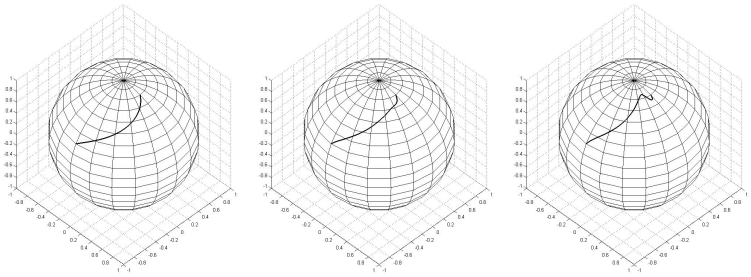

(a) $\varepsilon = 0.1$ (b) $\varepsilon = 0.8$ (c) $\varepsilon = 1.2$

Fig. 6: Head movement under the influence of a potential function and a constant friction term

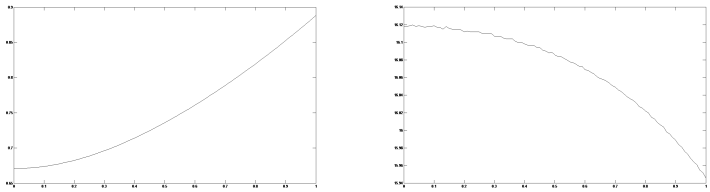

(a) Total Distance Traversed (b) Total Time Elapsed

Fig. 7: Distance and time as a function of ε.

certain region of the gaze-space. This is because of physical constraints that the eye ball cannot rotate to a certain position. We show that this can be achieved by a suitable choice of a potential function in conjunction with a friction term. Appropriate control of the potential function can be used to redirect the eye and head between points. We also show that, not very surprisingly, the friction term dampens the overshoot and reduces oscillations in the eye movement. Spontaneous head movements are constrained by a perturbation of the Listing's Law which allows for slight amounts of torsional movement. For a specific choice of the potential function, we show that rapid transfer of gaze between two gaze directions would require Listing's constraint to be violated. We propose that LISTING is restored at the end by vestibuloocular reflex, not studied in the paper. Using a similar choice of potential function, we show that rapid head movement would require introducing slight amount of torsion (ε slightly greater than 0). In summary, **an optimally chosen torsional component improves the transfer time for both the eye and the head,** perhaps at the cost of disorienting the target.

VI. Acknowledgement

The first author would like to acknowledge helpful advice from Dr. Steve Glasauer and Dr. Erich Schneider from Ludwig-Maximilians-University, München, Germany. This material is based upon work supported by the National Science Foundation under Grant No. 0523983. Any opinions, findings, and conclusions or recommendations expressed in this material are those of the author(s) and do not necessarily reflect the views of the National Science Foundation.

References

[1] Angelaki, D. and Hess, B. J. M., "Control of Eye Orientation: Where Does the Brain's Role End and the Muscle's Begin", Review Article, *European J. of Neuroscience*, vol. 19, pp. 1–10, 2004.

[2] Boothby, W. M., *An Introduction to Differentiable Manifolds and Riemannian Geometry*, CA: Academic-Press, 1986.

[3] Bullo, F. and Lewis, A. D., *Geometric Control of Mechanical Systems*, Springer-Verlag, 2004.

[4] Crawford, J. D., Ceylan, M. Z., Klier, E. M. and Guitton, D., "Three Dimensional Eye-Head Coordination During Gaze Saccades in the Primate", *J. Neurophysiol.*, vol. 81, pp. 1760–1782, 1999.

[5] Glasauer, S., "Current Models of the Ocular Motor System", *Neuro-Ophthalmology, Dev. Ophthalmology*, Basel, Karger, vol. 40, pp. 158–174, 2007.

[6] Martin, C. and Schovanec, L., "Muscle Mechanics and Dynamics of Ocular Motion", *J. of Mathematical Systems, Estimation and Control*, vol. 8, pp. 1–15, 1998.

[7] Medendorp, W. P., Gisbergen, J. A. M. Van., Horstink, M. W. I. M. and Gielen, C. C. A. M., "Donder's Law in Torticollis", *J. Neurophysiology*, vol. 82, pp. 2833–2838, 1999.

[8] Murray, R. M., "Nonlinear Control of Mechanical Systems: A Lagrangian Perspective", *Annu. Rev. Control*, vol. 21, pp. 31–45, 1997.

[9] Polpitiya, A. D., Dayawansa, W. P., Martin, C. F., and Ghosh, B. K., "Geometry and Control of Human Eye Movements", *IEEE Transactions in Automatic Control*, vol. 52, no. 2, pp. 170–180, Feb. 2007.

[10] Radau, P., Tweed, D. and Vilis, T., "Three Dimensional Eye head and Chest Orientations Following Large Gaze Shifts and the Underlying Neural Strategies", *J. Neurophysiol.*, vol. 72, pp. 2840–2852, 1994.

[11] Raphan, T., "Modeling Control of Eye Orientation in Three Dimension – Role of Muscle Pulleys in Determining Saccadic Trajectory", *J. Physiol.*, vol. 79, pp. 2653–2667, 1998.

[12] Robinson, D., "The Mechanics of Human Saccadic Eye Movement", *J. Physiol.*, vol. 174, pp. 245–264, 1964.

[13] Tweed, D. and Villis, T., "Geometric Relations of Eye Position and Velocity Vectors During Saccades ", *Vision Res.*, vol. 30, pp. 111–127, 1990.

[14] Tweed, D., "Three Dimensional Model of the human Eye-Head Saccadic System", *J. Neurophysiology*, vol. 77, pp. 654–666, 1997.

[15] Tweed, D., Haslwanter, T. and Fetter, M., "Optimizing Gaze Control in Three Dimensions", *Science*, vol. 281(28), pp. 1363–1365, Aug., 1998.